

Optical Phase Control of an Optically Injection-Locked FET Microwave Oscillator

RONALD D. ESMAN, MEMBER, IEEE, LEW GOLDBERG, AND J. F. WELLER

Abstract — A simple technique is proposed and demonstrated for controlling the phase of an optically injection-locked 7.2 GHz FET oscillator. The relative phase ϕ between the oscillator and the optically injected locking signal is adjusted by optically tuning the oscillator frequency. Locking characteristics described include locking bandwidth (2.6 MHz), phase tuning range (187°), phase modulation ($\beta = 0.69$ at 500 kHz), and optical tuning (125 MHz).

I. INTRODUCTION

OPTICALLY injection-locked microwave oscillators are attractive for airborne and space applications since the locking signal can be distributed using lightweight optical fiber. The growing availability of wide-bandwidth laser diodes has stimulated renewed interest [1], [2] in the optical injection locking technique. Using a directly modulated laser, FET oscillator locking has been demonstrated [3]–[5] at frequencies up to 3 GHz and in this work at 7.2 GHz. Higher locked frequencies have been reported but depend on mixing of two laser diodes [6] (9.6 GHz), laser harmonic generation and indirect injection [7] (10.2 GHz), or indirect injection and FET subharmonic locking [8] (21.5 GHz).

Potential applications, such as phased array radar and microwave power combining, require not only frequency-locked (coherent) sources but also individual source phase control. However, optical techniques for phase control have been limited to optically controlled varactors [9] and to fiber stretching [8] and fiber length switching techniques [10], [11]. These techniques suffer from a number of drawbacks, including limited phase shifts, discrete phase shifts, slow response, moderate to prohibitive insertion loss, high voltage requirement, and small phase modulation bandwidths, as well as the size and the weight of the additional components required.

Our approach is similar to that of Sato [12] on combined *electrical* injection locking and tuning where a phase-locked loop stabilizes a Gunn diode oscillator via oscillator frequency tuning by bias control. Also, Seeds *et al.* [13] have proposed an optical technique similar to the present ap-

Manuscript received October 24, 1988; revised April 28, 1989. This work was supported by the U.S. Office of Naval Technology program on electro-optics.

The authors are with the Naval Research Laboratory, Code 6570, Washington, DC 20375-5000.

IEEE Log Number 8929897.

proach but relying on an external optical intensity modulator.

In this paper we present and demonstrate a new optical technique for controlling the phase of an optically injection-locked oscillator that utilizes existing components, requires low power, allows for continuous phase tuning up to more than 180°, and exhibits a phase modulation bandwidth limited only by the locking bandwidth. The technique relies on the property of an injection-locked oscillator where its relative phase is determined by the difference between the free-running and injection frequencies, which in turn depends on the average incident optical power. Therefore, control of the relative phase is easily accomplished via control of laser diode bias.

Following a brief theoretical review and a short discussion of locking bandwidth, a description of the 7.2 GHz oscillator and of the injection locking setup is presented. We then discuss the experimental results, which include effects of optical illumination on the oscillator, locking bandwidth, and optical control of phase by varying both the injected frequency and the oscillator frequency.

II. THEORY

A. Results of Small-Signal Electrical Injection Locking

The principle of electrically injection-locked oscillators has been presented elsewhere [14], [15]. Optical injection locking differs only in the way in which the injection signal is inserted into the oscillator, that is, through photoconductive detection [16] in the FET. From small-signal electrical theory, the locking range Δf_m can be related to the injected power P_{inj} , the oscillator output power P_{opr} , and the oscillator external Q_{ext} by [14]

$$\Delta f_m = \frac{f_{\text{opr}}}{Q_{\text{ext}}} \sqrt{P_{\text{inj}}/P_{\text{opr}}} \quad (1)$$

Here, the optically shifted unlocked operating frequency of the oscillator, f_{opr} , corresponds to the natural frequency of the illuminated oscillator. Operating variables differ from unilluminated (conventional) free-running variables only in that they depend on the average optical power incident on the FET. It should be noted that P_{inj} is the equivalent electrical power generated by the absorbed optical signal.

Another important relevant equation for phase control relates the phase angle ϕ between the oscillator signal and the injected signal. Under the locked condition, $d\phi/dt = 0$ and [14], [15]

$$\phi = \arcsin(2\Delta f/\Delta f_m) \quad (2)$$

where $\Delta f = f_{\text{opr}} - f_{\text{inj}}$ is the optically controlled difference frequency between the operating frequency f_{opr} and the injected frequency f_{inj} and ϕ is limited to a range of 180° from -90° to 90° . The phase ϕ can then be optically adjusted by changing Δf via f_{opr} tuning. Tuning the oscillator frequency by optical illumination has been well documented in oscillators using FET's [4], [5], [17], [18] and is attributed to optically induced changes in the transistor transconductances [5] and capacitances [19].

We emphasize here that (1) and (2) are derived from small-signal analysis of a simple tuned circuit. Kurokawa [15] has pointed out that when nonlinear device reactance is taken into account, the locking range can increase and the phase range can extend beyond 180° .

B. Output of an Unlocked Oscillator at the Injected Frequency

The spectrum from an unlocked driven oscillator has been previously observed [6], [7], [15], [20], [21] and explained theoretically [22]. When the frequency of the injected signal is just outside of the locking range, many difference-frequency-spaced single-sided sidebands appear. The relative amplitude of each oscillator sideband as well as the component at the injected frequency is elegantly explained by Armand [22]. That is, even when the oscillator is out of lock, the oscillator spectrum contains a nonzero component at the injected signal frequency f_{inj} at some measurable relative phase ϕ . Outside of the locking range the relative power at f_{inj} is given by [22]

$$|S_{21}|^2 = \tan^2 \left[\frac{1}{2} \sin^{-1} \left(\frac{\Delta f_m}{2\Delta f} \right) \right] = \left[\frac{2\Delta f}{\Delta f_m} - \sqrt{\left(\frac{2\Delta f}{\Delta f_m} \right)^2 - 1} \right]^2 \quad (3)$$

and is plotted with the relative phase (eq. (2)) in Fig. 1. The relative phase of the f_{inj} component outside the locking range is left undetermined analytically since the exact model of the feedback circuit is not known in general.

C. Locking Bandwidth

A precise definition of the locking bandwidth can take several forms. The most common forms define the locking bandwidth as the difference between the frequencies at which

- the single-sided difference-frequency sidebands disappear, Δf_{ss} (emphasis on absolute lock);
- the response is $1/\sqrt{2}$ (-3 dB) of the response in the center of the locking range, $\Delta f_{3\text{dB}}$ (emphasis on locked signal content);
- the relative phase abruptly becomes independent of frequency, Δf_ϕ (emphasis on phase excursion).

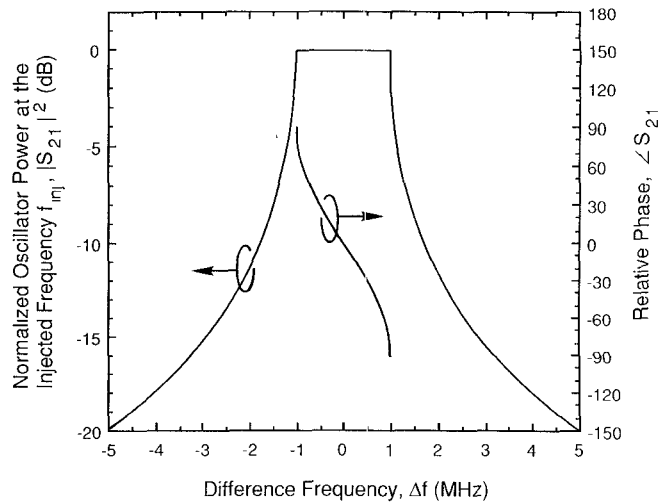


Fig. 1. Predicted transfer function of a locked and near-locked driven oscillator based on eqns. (2) and (3).

Equations (2) and (3) may be used to analytically determine the relationship between the magnitudes of the various locking bandwidths. For example, $\Delta f_{ss} = \Delta f_\phi = \Delta f_m$, whereas $\Delta f_{3\text{dB}} = (3/2\sqrt{2})\Delta f_m \cong 1.061 \Delta f_m$.

Due to the following practical considerations, in this work we measured the 3 dB locking bandwidth $\Delta f_{3\text{dB}}$. Jitter in the FET oscillator frequency f_{opr} , presumed to be primarily due to fluctuations in the optical signal coupled into the active region of the FET, introduces significant fluctuations in $|S_{21}|^2$ near the edges of the locking bandwidth where the response is sharply dependent on the difference frequency (see Fig. 1). As a result, the band edges appear jagged in the experimental traces that correspond to Fig. 1. With detection averaging, the corners in the response become reproducible, though slightly rounded, so that the 3 dB bandwidth then was the one which could be most easily determined from the measurement.

III. EXPERIMENTAL SETUP

A. The FET Oscillator Circuit

The microwave oscillator used in this work utilized an Avantek M106 GaAs FET. The transistor gate is $0.3 \times 250 \mu\text{m}$ while the source-drain separation is $3-4 \mu\text{m}$. For the illumination conditions discussed below, we estimate that 5–10 percent of the incident light is not blocked by the electrode metallization and that approximately 2×10^{14} photons/s are absorbed per milliwatt of incident optical power P_{opt} . The transistor is mounted in an unenclosed microstrip subassembly, which allows optical access. A 7.2 GHz oscillator with parallel-type feedback [23] is formed by series connecting a wire inductor between the drain terminal and a chip capacitor positioned on the gate terminal.

Along with the microstrip subcircuit, the complete oscillator, shown schematically in Fig. 2, also consists of coaxial components including a gate connector, a bias tee to a drain connector, and a double-stub tuner for impedance matching. A 20 dB attenuator isolates the oscillator from

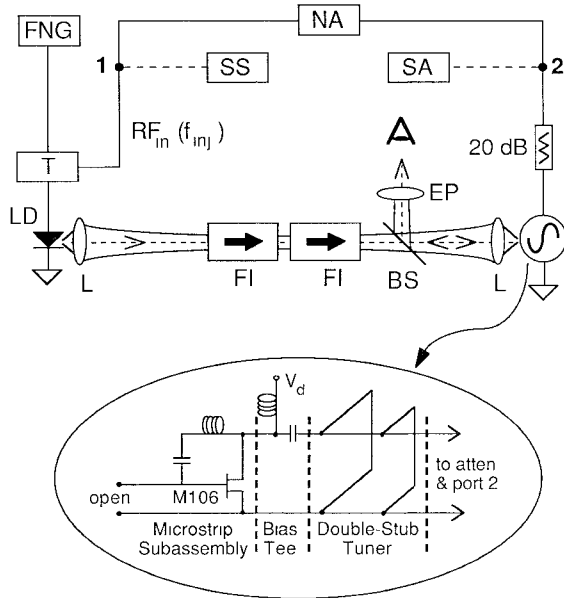


Fig. 2. Experimental setup. Either the network analyzer (NA) or the synthesized sweeper/spectrum analyzer (SS/SA) was connected to ports 1 and 2. The Faraday isolators (FI) provide about 60 dB of optical isolation. Laser diode bias and low-frequency direct modulation are provided by a function generator (FNG).

the load. The gate connector served as an open-circuit stub and allowed for coarse tuning by lengthening. However, the widest locking bandwidths and the most stable results were obtained by using only the open connector. The drain-source bias voltage was kept low (< 1.5 V) to avoid large voltage swings in this small-signal FET since, in this laboratory setup, a) the FET was not well heat sunk and b) gate biasing through a bias tee was prohibited due to the favorable characteristics with an open gate connection.

B. Optical and Electrical Configuration

In the experimental setup (Fig. 2) the high-speed laser diode [24] (LD) beam was collected by a $20\times$ lens (L), focused between the Faraday isolators (FI) and then focused on the gate of the FET. The laser threshold current I_{th} was 15 mA and was typically biased at 40 mA. The Faraday isolators prevent optical feedback to the LD, which is known to affect the RF response of LD's [2]. A beam splitter (BS) and eyepiece (EP) allow observation of the FET surface and incident laser spot.

In the following experiments the position of the ~ 10 μm diameter light spot, positioned to maximize the locking bandwidth, was at the bridge region where the gate contact meets the gate metallization. This interconnection bridge region also corresponds to where the optical signal had the greatest effect on the operating frequency. The enhanced optical sensitivity at the interconnecting bridge region has been previously observed in several FET devices [25] and may be due to the locally increased potential difference between the gate and the underlying conducting channel [25].

A synthesized sweeper/spectrum analyzer (SS/SA) pair or a network analyzer (NA), connected between ports 1

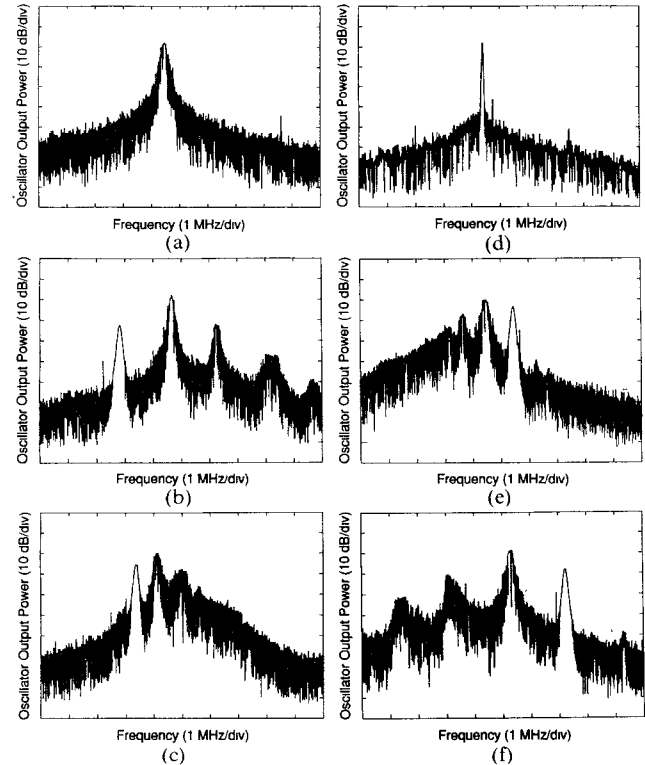


Fig. 3. Stages in the spectrum of the optically injected driven ET oscillator as the injected frequency is scanned near the locking range. The SA RBW is set to 100 kHz for all traces except (d), where RBW = 30 kHz. The center frequency on all traces is 7.123 GHz. (a) Free-running illuminated undriven oscillator. The oscillator line width is ~ 135 kHz in this 20 ms sweep. (b) $\Delta f \approx 2$ MHz; to compare to subsection IV-B, $|S_{21}|^2 \approx -14$ dB. (c) $\Delta f \approx 1$ MHz; $|S_{21}|^2 \approx -7.2$ dB. (d) Locked. (e) $\Delta f \approx -1$ MHz; $|S_{21}|^2 \approx -5.2$ dB. (f) $\Delta f \approx -2$ MHz; $|S_{21}|^2 \approx -9.5$ dB.

and 2 of the setup, provided the RF drive to the directly modulated laser and displayed RF data including oscillator spectra and RF throughput and phase (S_{21}) information. The NA is particularly helpful in displaying the 3 dB locking bandwidth and the associated phase tuning range.

IV. EXPERIMENTAL—EFFECTS OF INJECTED FREQUENCY TUNING

A. Oscillator Output Spectrum

Oscillator optical injection locking was observed by using the SS/SA. The oscillator was nominally operated near $V_d = 1$ V, corresponding to an operating frequency near 7.1 GHz, while the laser was modulated by an RF signal of $P_{LD} = -4.9$ dBm, corresponding to 100 μW peak variation in optical power incident on the FET. The SS modulation frequency f_{inj} driving the laser was varied around the oscillator operating frequency. When the oscillator was unlocked but f_{inj} was close to f_{opr} , the oscillator output spectra contained many single-sided sidebands very similar to those reported by others [6], [7], [15], [20], [21] and theoretically explained by Armand [22] for an unlocked driven oscillator. Fig. 3(a) shows the spectrum of the illuminated FET oscillator with the laser modulation turned off. Fig. 3(b)–(f) shows the evolution of the spectrum as the injected frequency (with P_{LD} constant) is increased

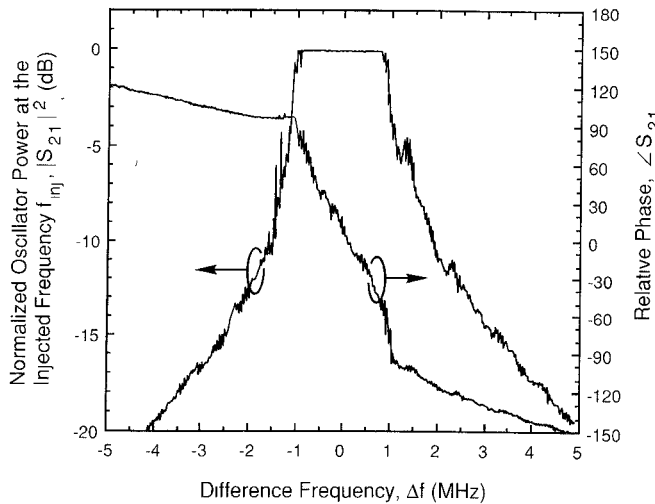


Fig. 4. Squared magnitude and relative phase of S_{21} versus difference frequency Δf , where $f_{\text{opr}} = 7.123$ GHz is taken to be the frequency at the center of the locking band. The oscillator output power is 3 dBm while $P_{\text{LD}} = -7.5$ dBm. Compare to Fig. 1.

from too low for locking to take place, to within the locking range, to too high for locking. Note that, except for the locked case (Fig. 3(d)), the SA resolution bandwidth (RBW) was approximately equal to the measured oscillator line width. Useful traces with a narrower SA RBW were prevented by the associated longer sweep time and oscillator frequency jitter. When f_{inj} was tuned within the locking range (Fig. 3(d)), all sidebands disappeared, frequency jitter was eliminated, and oscillator FM noise was significantly reduced, consistent with the injection locking process.

B. Injected Signal Transfer Characteristics Versus Injected Frequency

Additional characterization of the oscillator optical locking performance was provided by the NA measurement of S_{21} . Here, we give $|S_{21}|^2$ normalized to the maximum $|S_{21}|^2$ which occurs during lock when all of the oscillator power is at the injected frequency. Note that the normalized $|S_{21}|^2$ is also the normalized oscillator power at f_{inj} . The squared magnitude and phase of S_{21} are plotted versus the difference frequency in Fig. 4 for $P_{\text{opt}} = 1.2$ mW and incident microwave power driving the laser $P_{\text{LD}} = -7.5$ dBm. The S_{21} response compares well with the corresponding small-signal theory plot of Fig. 1. Note the characteristic flat top variation where in the flat portion of the curve all of the oscillator power is at the injected frequency. Both the squared magnitude and phase of S_{21} show residual jaggedness due to oscillator frequency jitter discussed above, even after numerical averaging has reduced the effective NA detection bandwidth to ~ 1 kHz.

For the operating conditions of Fig. 4, a 2.0 MHz 3 dB locking bandwidth was observed. For comparison, the same locking bandwidth was observed in conventional microwave injection locking experiments where the locking signal ($P_{\text{inj}} \approx -46$ dBm) is directly injected at port 2. The 3 dB phase tuning range $\phi_{3\text{dB}}$, defined by the difference in

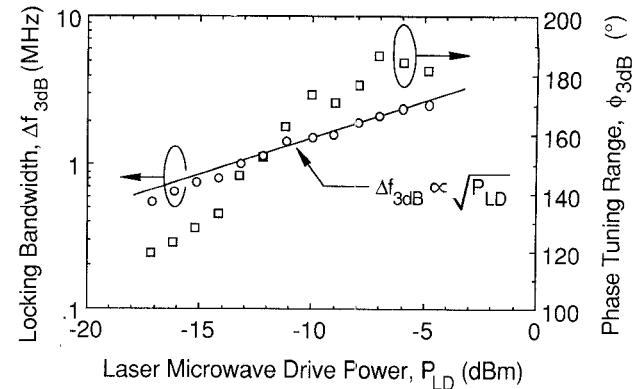


Fig. 5. Locking bandwidth (○) and phase tuning range (□) versus laser microwave drive power for $P_{\text{opt}} = 1.2$ mW. A calculated curve where the $\Delta f_{3\text{dB}}$ is proportional to the square root of the laser drive power is shown for comparison.

phase at the -3 dB points of $|S_{21}|^2$, was about 184° . Since the path lengths for the NA were not equalized, this value was obtained by reducing the directly measured value by $2.4^\circ/\text{MHz}$ to account for the length (~ 2 m) of the experimental setup.

Plots similar to those of Fig. 4 were generated at various P_{LD} 's, and the resulting 3 dB locking bandwidths and corrected phase ranges are plotted in Fig. 5. The locking bandwidth-drive power characteristic compares well with the calculated square-root dependence of (1) with the maximum locking bandwidth of 2.6 MHz at $P_{\text{LD}} = -4.9$ dBm. An indication of the degree of averaging and amount of frequency jitter is given by the ratio of the 3 dB to the 0.1 dB locking bandwidth; for most measurements it was ~ 1.5 , which compares to 1.06—the ratio $\Delta f_{3\text{dB}}/\Delta f_m$ in the ideal case with no averaging (see subsection II-C).

The maximum $\phi_{3\text{dB}}$ was 187° at -7.1 dBm. For lower drive levels phase changes exceeding 180° were always possible (see Fig. 4), but only a fraction of the change was within the 3 dB locking bandwidth. Even though the measurement of $\phi_{3\text{dB}}$ relies on a seemingly arbitrary definition, the 3 dB locking bandwidth never extended beyond the rather abrupt bends of the phase characteristic near the band edge and so never overestimates the available phase tuning. For some conditions, especially at higher laser drive levels (> -8 dBm), $\phi_{3\text{dB}}$ extends beyond 180° and may be due to device reactive nonlinearities that can lead to phase shifts greater than 180° .

V. EXPERIMENTAL—EFFECTS OF OPTICALLY CONTROLLED OSCILLATOR FREQUENCY TUNING

A. Oscillator Frequency Tuning by Optical Illumination

To determine the effect of optical illumination on f_{opr} , the oscillator output was observed on the SA as P_{opt} was varied by changing the bias current of the unmodulated laser. Fig. 6 shows the dependence of f_{opr} on P_{opt} for various FET drain bias voltages V_d . For $V_d = 0.96$ V, the oscillator could be tuned up to 125 MHz (~ 1.8 percent of f_{opr}) by adjusting P_{opt} . The optical tuning characteristics in

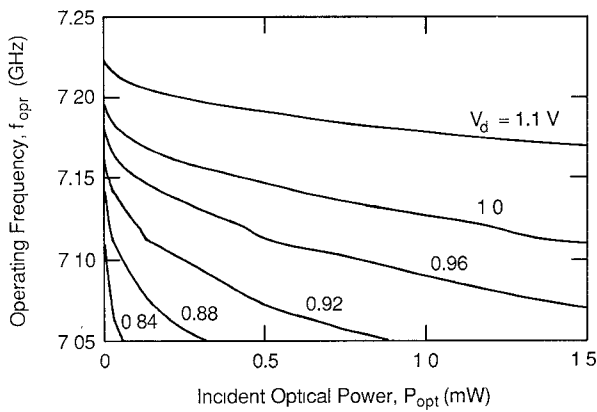


Fig. 6. Operating frequency f_{opr} versus incident optical power P_{opt} at various FET drain voltages. The oscillator output power is 3 dBm. The oscillator was typically operated where the frequency tuning coefficient was 30–40 MHz/mW.

Fig. 6 are consistent with previously published models [5] and results [18], [26]. That is, for unmodulated illumination, as the optical power increases, the optically injected carriers reduce the FET gate depletion depth and so the gate–source capacitance increases, which leads to a decreased resonance frequency. For the present application it is significant that the optical tuning range is larger than the typical locking bandwidths observed, so that the full phase shift given by (2) could be achieved.

Besides phase control and modulation to be presented here, optical tuning has two related applications. First, the relatively large tuning range makes it possible to effectively extend the locking bandwidth by optically tuning the oscillator operating frequency so that it tracks changes in the injected frequency. Second, optical tuning can be useful for maintaining the locking condition by compensating for drift of the oscillator operating frequency.

B. Injected Signal Transfer Characteristics Versus Optical Illumination

Optical injection locking with phase control was demonstrated by varying the bias current to the laser to change the average optical power without significantly changing the microwave optical modulation depth or the effective optically injected microwave signal power level. P_{opt} is changed linearly with bias current over small (few mA) variations in laser current while the NA frequency is kept constant. Fig. 7 shows how S_{21} at 7.127 GHz changes as the optical power incident on the FET P_{opt} varied from 0.95 to 1.175 mW, where $P_{LD} = -4.9$ dBm and the oscillator output power $P_{opr} = 3$ dBm. The shapes of the squared magnitude and phase curves in Fig. 7 are similar to those in Fig. 1 and Fig. 4, indicating both that a) these locking characteristics are affected similarly by a change in f_{inj} or by optically induced changes in f_{opr} and b) the small-signal theory used to derive Fig. 1 is an accurate representation of the present experiments.

Although in most solid-state devices changes in incident optical power can be accompanied by changes in signal amplitude [5], [18], [26], Fig. 7 shows that a negligible

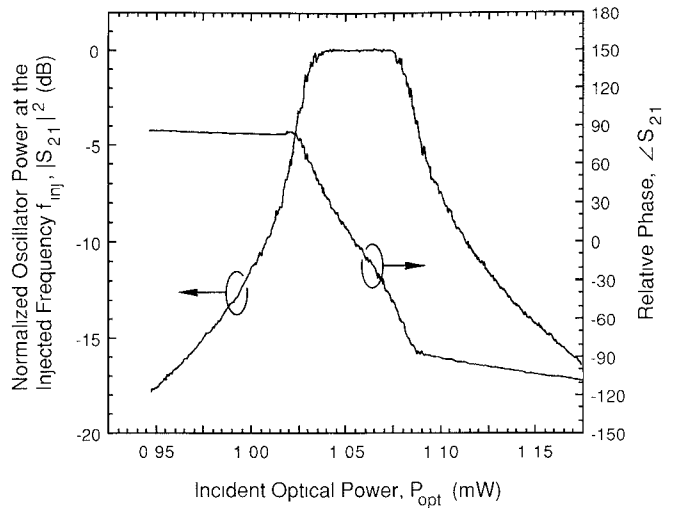


Fig. 7. Squared magnitude and relative phase of S_{21} versus average incident optical power with $f_{inj} = 7.127$ GHz. The oscillator exhibits a $\phi_{3db} = 154^\circ$ phase change within the 3 dB locking bandwidth, which corresponds to $I_{pp} = 1.05$ mA and $P_{opt,pp} = 58$ μ W. Compare to Figs. 1 and 4.

change in output power was observed over the locking range. In fact, in separate experiments, the oscillator output power did not change by more than ~ 1 dB, even when the incident power was varied from ~ 20 μ W to 1.2 mW. These results indicate that, for this oscillator configuration, gain variations due to illumination are negligible. This is consistent with the expected conditions of an invariant load line and an internal gate bias voltage self-adjusted well away from the pinch-off voltage, near which the effects of illumination are enhanced [5], [26].

C. Optically Controlled Phase Modulation

To demonstrate phase modulation, the LD was biased and modulated directly by the function generator via the dc port of the bias T, which had a flat frequency response to 1 MHz. An example of low-frequency phase modulation is shown in Fig. 8(a), where current to the laser was changed sinusoidally at 25 Hz. While the laser was biased at 32.0 mA, peak-to-peak laser bias current modulation of $I_{pp} = 0.4$ mA ($P_{opt,pp} = 14$ μ W) yielded peak-to-peak phase modulation of more than 104° while simultaneously maintaining an output magnitude flat to within 0.3 dB. Modulation speed was limited mainly by the NA sweep speed (here, 200 ms).

For phase modulation at higher frequencies, the injection-locked oscillator RF spectrum was observed on the SA (Fig. 8(b)), with the laser $I_{pp} = 1.4$ mA at 500 kHz. The ratio of the first sidebands to the carrier is 0.37, giving a modulation index $\beta = 0.69$ or a peak-to-peak phase modulation of 78.5° . Higher modulation depths (larger current excursions) resulted in asymmetric sidebands followed by spurious peaks appearing near the center of the band (loss of lock). Phase modulation to 1 MHz was observed but distortion-free phase modulation was limited to a modulation index of less than 0.05. For the conditions of Fig.

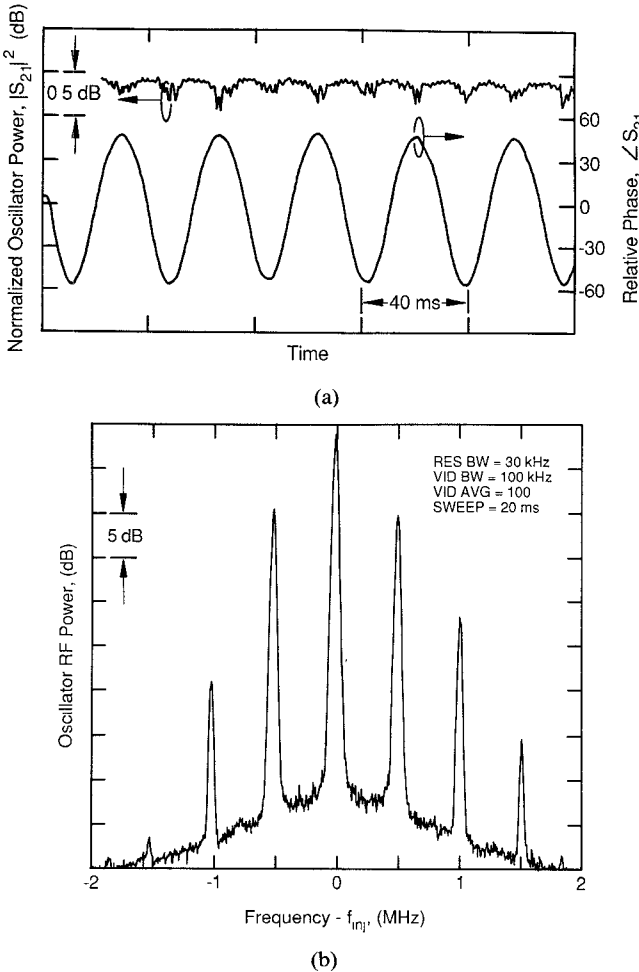


Fig. 8. (a) S_{21} as a function of time with low frequency (25 Hz) laser bias current modulation— $I_{pp} = 0.4$ mA. (b) Oscillator RF spectrum about $f_{inj} = 7.131$ GHz with high-frequency (500 kHz) modulation of the laser bias current.

8(b), the locking bandwidth of ~ 2 MHz was measured. Similar to the case of other microwave drive and laser bias levels, the phase modulation bandwidth was well correlated to the locking bandwidth of the laser–oscillator pair.

VI. CONCLUSION

Optical injection locking characteristics for both injection frequency tuning and optically controlled oscillator frequency tuning have been shown to agree with those predicted by small-signal injection locking theory. An injection locking bandwidth up to 2.6 MHz and a phase tuning range up to 187° have been observed.

We have demonstrated for the first time the use of optical power as a means of tuning a FET oscillator operating frequency to simultaneously control the phase of the oscillator output relative to the phase of the injection locking signal. The technique relies on laser bias control, requires very few additional components, offers continuous phase modulation over more than 100° for low frequencies, allows for low-index modulation at frequencies up to the locking bandwidth, and is suited for fiber-optic control of remote microwave oscillators. The technique

allows for compensation of difference frequency variations by simultaneous optical tuning (in a phase-lock loop) and so can be used either to extend the effective locking bandwidth by tracking changes in the injected frequency or to counteract oscillator drift.

ACKNOWLEDGMENT

One of the authors (R.D.E.) would like to thank Dr. C. Rauscher of NRL for helpful discussions regarding FET oscillator construction and operation.

REFERENCES

- [1] P. R. Herczfeld *et al.*, "Optically controlled PIN microwave phase-shifter," *SPIE*, vol. 545, (Optical Technology for Microwave Applications II), pp. 39–44, 1985.
- [2] D. C. Buck and M. A. Cross, "Optical injection locking of FET oscillators using fiber optics," in *IEEE MTT-S Int. Microwave Symp. Dig.*, 1986, pp. 611–614.
- [3] H. W. Yen and M. K. Barnoski, "Optical injection locking and switching of transistor oscillators," *Appl. Phys. Lett.*, vol. 32, pp. 182–184, 1978.
- [4] A. A. Salles and J. R. Forrest, "Initial observations of optical injection locking of GaAs metal semiconductor field effect transistor oscillators," *Appl. Phys. Lett.*, vol. 38, pp. 392–394, 1981.
- [5] A. A. A. De Salles, "Optical control of GaAs MESFET's," *IEEE Trans. Microwave Theory and Tech.*, vol. MTT-31, pp. 812–820, 1983.
- [6] L. Goldberg, C. Rauscher, J. F. Weller, and H. F. Taylor, "Optical injection locking of X-band FET oscillator using coherent mixing of GaAlAs lasers," *Electron. Lett.*, vol. 19, pp. 848–850, 1983.
- [7] A. S. Daryoush and P. R. Herczfeld, "Indirect optical injection-locking of multiple X-band oscillators," *Electron. Lett.*, vol. 22, pp. 133–134, 1986.
- [8] A. S. Daryoush, P. R. Herczfeld, R. Glatz, and A. P. S. Khanna, "Phase and frequency coherency of multiple optically synchronized 20 GHz FET oscillators for satellite communications," in *IEEE MTT-S Int. Microwave Symp. Dig.*, 1987, pp. 823–826.
- [9] L. R. Brothers, Jr., and C. H. Cox III, "A high-speed phase shifter based on optical injection," in *IEEE MTT-S Int. Microwave Symp. Dig.*, 1987, pp. 819–822.
- [10] R. A. Soref, "Programmable time-delay devices," *Appl. Opt.*, vol. 23, pp. 3736–3737, 1984.
- [11] B. Lagerstrom *et al.*, "Integrated-optic delay line processor," in *Proc. Opt. Fiber Conf.*, 1986, paper WK2.
- [12] G. Sato, "Stabilized oscillators by using injection locking and phase-locked loop," *Electron. Commun. Japan*, vol. 54-B, pp. 59–65, 1971.
- [13] A. J. Seeds, I. D. Blanchflower, N. J. Gomes, G. King, and S. J. Flynn, "New developments in optical control techniques for phased array radar," in *IEEE MTT-S Int. Microwave Symp. Dig.*, 1988, pp. 905–908.
- [14] R. Adler, "A Study of locking phenomena in oscillators," *Proc. IRE*, vol. 34, pp. 351–357, 1946.
- [15] K. Kurokawa, "Injection locking of microwave solid state oscillators," *Proc. IEEE*, vol. 61, pp. 1386–1410, 1973.
- [16] J. C. Gammel and J. M. Ballantyne, "The OPFET: A new high speed optical detector," in *Proc. IEEE IEDM* (New York) 1978, pp. 120–123.
- [17] B. Loriou, J. Guena, and J. F. Sautereau, "Optically frequency modulated GaAs MESFET oscillator," *Electron. Lett.*, vol. 17, pp. 901–902, 1981.
- [18] H. Mizuno, "Microwave characteristics of an optically controlled GaAs MESFET," *IEEE Trans. Microwave Theory Tech.*, vol. MTT-31, pp. 596–600, 1983.
- [19] J. R. Forrest and A. J. Seeds, "Analysis of the optically controlled IMPATT (Opcad) oscillator," *Solid-State and Electron Devices*, vol. 3, pp. 161–169, 1979.
- [20] H. W. Yen, "Optical injection locking of Si IMPATT oscillators," *Appl. Phys. Lett.*, vol. 36, pp. 680–683, 1980.
- [21] H. L. Stover, "Theoretical explanation for the output spectra of unlocked driven oscillators," *Proc. IEEE*, vol. 54, pp. 310–311, 1966.

- [22] M. Armand, "On the output spectrum of unlocked driven oscillators," *Proc. IEEE*, vol. 57, pp. 798-799, 1969.
- [23] C. Rauscher, "Large-signal technique for designing single-frequency and voltage-controlled GaAs oscillators," *IEEE Trans. Microwave Theory Tech.*, vol. MTT-29, pp. 293-304, 1981.
- [24] Ortel Laser Diode, Model SL1000, Ortel Corp., 2015 West Chestnut Street, Alhambra, California 91803.
- [25] T. F. Carruthers, W. T. Anderson, and J. F. Weller, "Optically induced, spatially resolved backgating transients in GaAs FETs," in *Proc. IEEE IEDM* (Washington, DC) 1985, pp. 106-109.
- [26] R. N. Simons, "Microwave performance of an optically controlled AlGaAs/GaAs high electron mobility transistor and GaAs MESFET," *IEEE Trans. Microwave Theory Tech.*, vol. MTT-35, pp. 1444-1455, 1987.



Lew Goldberg received the B.S. degree in electrical engineering from Tufts University, Medford, MA, in 1973, the M.S. degree from Carnegie Mellon University, Pittsburgh, PA, and the Ph.D. degree in applied physics from the University of California, San Diego, in 1979. He remained at UCSD to teach until 1980.

His doctoral thesis research was conducted in the area of guided wave optics and semiconductor devices. Since 1980 he has been with the Naval Research Laboratory, Washington, DC, working on semiconductor laser properties, optical microwave transmission, high-power diffraction-limited laser diode sources, and nonlinear optical mixing for frequency conversion of laser diode emission.

Dr. Goldberg is a member of the Optical Society of America and the American Physical Society.

✖



Ronald D. Esman (S'82-M'85) was born in Kalamazoo, MI, on April 30, 1959. In 1981, he received the B.A. degree (magna cum laude) in physics and mathematics from Kalamazoo College, Kalamazoo, MI. He received the M.S. and D.Sc. degrees in electrical engineering from Washington University, St. Louis, MO, in 1983 and 1986, respectively.

In 1980, he interned at the Oak Ridge National Laboratory, Oak Ridge, TN, where his research included characterization and passivation of polycrystalline Si solar cells. While at Washington University he was a Research Assistant in the Optoelectronics Laboratory, where his work included the fabrication, large-signal analysis, and characterization of high-speed electroabsorption avalanche photodetectors. In 1984, he was with Computer Services Kaisha (CSK), Tokyo, Japan, working on write and read techniques for laser memory cards. In 1986 he joined the Naval Research Laboratory, Washington, DC, where he is working in the fields of high-speed optoelectronics, optical-microwave interactions, semiconductor laser noise and spectral characteristics, and fiber optics.

Dr. Esman is a member of Sigma Xi, Phi Beta Kappa, and the Optical Society of America.

✖



J. F. Weller received the B.S. degree in physics from Xavier University, Cincinnati, OH, in 1960 and the M.S. and Ph.D. degrees in physics from American University, Washington, DC, in 1968 and 1972 respectively.

He joined the Naval Research Laboratory, Washington, DC, in 1960, where he began work on radiation damage in semiconductor devices. Since then he has been active in areas of quantum electronics, ultrasonics, and fiber optics. His research interests have included rare earth spectroscopy in glasses, glass lasers, nonlinear optics, optical interactions with acoustic waves, laser diodes, and nonlinear optics. He is presently Head of the Optical Techniques Branch, which is involved in fiber sensors, guided wave technology, laser diodes and arrays, and picosecond optical probing.

Dr. Weller is a member of the American Physical Society and the Optical Society of America.